Contribution from the Dipartimento di Chimica Inorganica, Chimica Fisica e Chimica dei Materiali, University of Torino, Via P. Giuria 7, 10125 Torino, Italy, and Dipartimento di Chimica "G. Ciamician", University of Bologna, Via F. Selmi 2, 40126 Bologna, Italy

Dynamic Processes in the Solid State. Proton Relaxation Studies and Potential Energy Barrier Calculations for (arene)$M(CO)_3$ Species. X-ray Crystal Structures of (1,2,3-$C_6H_3Me_3$)$Cr(CO)_3$ and (1,2,4,5-$C_6H_2Me_4$)$Cr(CO)_3$

Silvio Aime,*[1a] Dario Braga,*[1b] Roberto Gobetto,[1a] Fabrizia Grepioni,[1b] and Alessandra Orlandi[1a]

Received June 15, 1990

The dynamic behavior in the solid state of (C_6Me_6)$Cr(CO)_3$ (**1**), (1,2,3-$C_6H_3Me_3$)$Cr(CO)_3$ (**2**), and (1,2,4,5-$C_6H_2Me_4$)$Cr(CO)_3$ (**3**) has been investigated by means of variable-temperature ^1H spin-lattice relaxation time T_1 measurements and potential energy barrier calculations. Structural characterization of **2** and **3** at room temperature by single-crystal X-ray diffraction has been carried out. Crystal data: **2**, space group $P2_1/n$, a = 7.289 (4) Å, b = 13.114 (4) Å, c = 12.526 (3) Å, β = 97.64 (4)°, V = 1186.7 Å^3, Z = 4; **3**, space group $P2_1/n$, a = 8.985 (1) Å, b = 12.527 (2) Å, c = 9.011 (1) Å, β = 118.22 (1)°, V = 1275.7 Å^3, Z = 4. It is found that, in all cases, the lowest energy dynamic process involves rotation of the methyl groups (E_a = 2-6 kJ/mol). Facile reorientation of the C_6Me_6 fragment in **1** is also detected (E_a = 25.9 kJ/mol) in good agreement with the results of potential energy barrier calculations. For **2** and **3**, it is shown that reorientation, at room temperature, of the arene fragments is forbidden by the crystal packing, while large amplitude motions appear to be responsible for the additional modulation detected in the log T_1 versus $10^3/T$ plots. The drastic reduction of T_1 observed for **2** and **3**, as the temperature is increased to ca. 333 K, is interpreted in terms of an order/disorder phase transition associated with full rotational freedom of the arenes or of the entire molecules. Support for this observation comes from the behavior of the diffraction patterns of the two species with temperature and from DSC measurements.

Proton relaxation times T_1 provide an experimental route to the study of molecular motions in the solid state.[2] Several organometallic species (such as cyclopentadienyl derivatives, (C_4H_4)$Fe(CO)_3$, (C_6H_6)$Cr(CO)_3$,[3i] etc.) have been studied by this technique.[3]

It has also been shown that information on such motions can be obtained from X-ray structural data, yielding values of the potential energy barriers in good agreement with those evaluated from the spectroscopic measurements.[4]

Recently, it has been reported that the motion of the CO ligands is responsible for the broadened features observed in the ^{13}CO resonances in the CP-MAS spectra of (C_6H_5Me)$Cr(CO)_3$ and of (C_6H_5Me)$Mo(CO)_3$.[5] However, this suggestion was found to be not consistent with the values of the potential energy barriers computed on the basis of the crystallographic data available for these compounds.[6] These calculations indicated that free rotation of the toluene fragment or of the $(CO)_3$ group around the coordination axis is not possible at room temperature.[4b,6b] On the other hand, the shape of the potential energy profiles suggested that large amplitude librational motions of both C_6H_5Me and $(CO)_3$ groups were responsible for the modulation of the carbon-hydrogen interaction, thus causing the observed broadening behavior of the carbonyl resonances in their variable-temperature spectra. In this paper, we report the proton log T_1 behavior as a function of the temperature for the complexes (C_6Me_6)$Cr(CO)_3$ (**1**), (1,2,3-

Table I. Relevant Bond Distances (Å) and Angles (deg) for **2** and **3**

2		**3**	
Cr-C(1)	1.81 (1)		1.830 (2)
Cr-C(2)	1.82 (1)		1.830 (2)
Cr-C(3)	1.83 (1)		1.838 (2)
Cr-C(4)	2.22 (1)		2.226 (2)
Cr-C(5)	2.20 (1)		2.203 (2)
Cr-C(6)	2.21 (1)		2.230 (2)
Cr-C(7)	2.22 (1)		2.232 (2)
Cr-C(8)	2.24 (1)		2.201 (2)
Cr-C(9)	2.24 (1)		2.235 (2)
C(1)-O(1)	1.15 (1)		1.152 (2)
C(2)-O(2)	1.16 (1)		1.162 (2)
C(3)-O(3)	1.15 (1)		1.147 (2)
C(4)-C(5)	1.38 (1)		1.401 (3)
C(5)-C(6)	1.42 (1)		1.417 (3)
C(6)-C(7)	1.39 (1)		1.400 (2)
C(7)-C(8)	1.40 (1)		1.420 (2)
C(8)-C(9)	1.40 (1)		1.399 (2)
C(4)-C(9)	1.39 (1)		1.421 (2)
C(7)-C(10)	1.51 (1)	C(4)-C(11)	1.498 (3)
C(8)-C(11)	1.51 (1)	C(6)-C(12)	1.511 (3)
C(9)-C(12)	1.50 (1)	C(7)-C(13)	1.503 (3)
		C(9)-C(10)	1.506 (3)
Cr-C(1)-O(1)	178 (1)		177.6 (2)
Cr-C(2)-O(2)	179 (1)		179.6 (1)
Cr-C(3)-O(3)	178 (1)		178.2 (2)
C(1)-Cr-C(2)	87.6 (3)		89.2 (1)
C(1)-Cr-C(3)	89.7 (3)		90.4 (1)
C(2)-Cr-C(3)	89.0 (3)		89.0 (1)
C(4)-C(5)-C(6)	120 (1)		122.4 (2)
C(5)-C(6)-C(7)	120 (1)		119.2 (2)
C(6)-C(7)-C(8)	120 (1)		118.0 (2)
C(7)-C(8)-C(9)	120 (1)		123.3 (3)
C(8)-C(9)-C(4)	119 (1)		118.2 (1)
C(9)-C(4)-C(5)	121 (1)		118.9 (2)
C(6)-C(7)-C(10)	119 (1)	C(4)-C(9)-C(10)	121.4 (2)
C(10)-C(7)-C(8)	121 (1)	C(10)-C(9)-C(8)	120.4 (2)
C(7)-C(8)-C(9)	121 (1)	C(5)-C(4)-C(11)	119.6 (2)
C(11)-C(8)-C(9)	119 (1)	C(11)-C(4)-C(9)	121.6 (2)
C(8)-C(9)-C(11)	122 (1)	C(5)-C(6)-C(12)	119.0 (2)
C(12)-C(9)-C(4)	118 (1)	C(12)-C(6)-C(7)	121.7 (2)
		C(6)-C(7)-C(13)	122.7 (2)
		C(13)-C(7)-C(8)	119.2 (2)

(1) (a) University of Torino. (b) University of Bologna.
(2) Fyfe, C. A. *Solid State NMR for Chemists*; CFC Press: Guelph, Ontario, Canada, 1983.
(3) (a) Holm, C. H.; Ibers, J. A. *J. Chem. Phys.* **1959**, *30*, 885. (b) Anderson, S. E. *J. Organomet. Chem.* **1974**, *71*, 263. (c) Gilson, D. F. R.; Gomez, G.; Butler, I. S.; Fitzpatrick, P. J. *Can. J. Chem.* **1983**, *61*, 737. (d) Butler, I. S.; Fitzpatrick, P. J.; Gilson, D. F. R.; Gomez, G.; Shaver, A. *Mol. Cryst. Liq. Cryst.* **1981**, *71*, 213. (e) Harvey, P. D.; Butler, I. S.; Gilson, D. F. R. *Inorg. Chem.* **1986**, *25*, 1009. (f) Campbell, A. J.; Fyfe, C. A.; Harold-Smith, D.; Jeffrey, K. R. *Mol. Cryst.* **1976**, *36*, 1. (g) Cottrell, C. E.; Fyfe, C. A.; Senoff, C. V. *J. Organomet. Chem.* **1972**, *43*, 203. (h) Campbell, A. J.; Cottrell, C. E.; Fyfe, C. A.; Jeffrey, K. R. *Inorg. Chem.* **1976**, *15*, 1321. (i) Delise, P.; Allegra, G.; Monaschi, E. R.; Chierico, A. *J. Chem. Soc., Faraday Trans. 2* **1975**, *71*, 207.
(4) (a) Braga, D.; Gradella, C.; Grepioni, F. *J. Chem. Soc., Dalton Trans.* **1989**, 1721. (b) Braga, D.; Grepioni, F. *Polyhedron* **1990**, *1*, 53. (c) Braga, D.; Grepioni, F.; Johnson, B. F. G.; Lewis, J.; Martinelli, M. *J. Chem. Soc., Dalton Trans.* **1990**, 1847. (d) When E_a is compared with ΔE values, it should be kept in mind that the activation energy is a mean value measured in a broad temperature range, while the potential energy barriers are dependent on the temperature at which diffraction data were collected. Since the activation energy integrates several effects (including correlated and uncorrelated jumping motion), one can expect to obtain only the same orders of magnitude for these two quantities.
(5) Wagner, G. W.; Hanson, B. E. *Inorg. Chem.* **1987**, *26*, 2019.
(6) (a) van Meurs, F.; van Konigsveld, H. J. *J. Organomet. Chem.* **1977**, *131*, 423; (b) Braga, D.; Grepioni, F. *J. Chem. Soc., Dalton Trans.* **1990**, 3143.

0020-1669/91/1330-0951$02.50/0

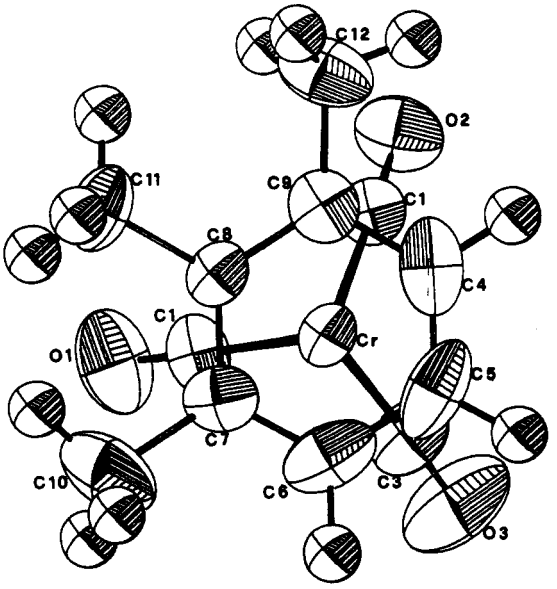

Figure 1. ORTEP projection of $(1,2,3\text{-}C_6H_3Me_3)Cr(CO)_3$ (**2**) showing 50% thermal ellipsoids.

$C_6H_3Me_3)Cr(CO)_3$ (**2**), and $(1,2,4,5\text{-}C_6H_2Me_4)Cr(CO)_3$ (**3**). The potential energy (PE hereafter) barriers to arene and tricarbonyl reorientation are computed by using the atom–atom pairwise potential energy method. The structures of **2** and **3** have been determined by single-crystal X-ray diffraction, while in the case of **1**, data available in the literature[7] have been used. The main structural features of $(1,2,3\text{-}C_6H_3Me_3)Cr(CO)_3$ and of $(1,2,4,5\text{-}C_6H_2Me_4)Cr(CO)_3$ are also discussed.

Results and Discussion

Crystal and Molecular Structures of $(1,2,3\text{-}C_6H_3Me_3)Cr(CO)_3$ (2) and $(1,2,4,5\text{-}C_6H_2Me_4)Cr(CO)_3$ (3). The structures of the two species are closely related and will be discussed together. ORTEP views of **2** and **3** are reported in Figures 1 and 2, respectively, together with the labeling schemes. Relevant structural parameters are grouped in Table I. Both molecules lie in general position in the respective unit cells. The two molecules adopt a staggered conformation. This conformation appears to be generally preferred to the eclipsed one in the family of (arene)$M(CO)_3$ species.[8] The eclipsed conformation is seen only for $(C_6H_5Me)Cr(CO)_3$[6a] [but note that $(C_6H_5Me)Mo(CO)_3$ is staggered],[6b] for the isostructural pair $(C_6Et_6)M(CO)_3$ (M = Cr, Mo)[9] and for $(1,3,5\text{-}C_6H_3Me_3)Mo(CO)_3$.[10] On the other hand, the difference in energy between the two conformations is very small, as demonstrated by extended Hückel calculations in $(C_6H_6)Cr(CO)_3$ (1.2 kJ/mol).[11] In the presence of such a low barrier, the intermolecular (packing) interactions can easily dominate the conformational choice in the solid state. However, the staggered conformations for **2** and **3** also achieve the least possible interaction between the Me groups and the underlying COs. Finally, it should be noticed that the Me and CO groups in **2** deviate (on the average) ca. 5° from the precise staggered geometry.

The C_6 rings are strictly planar in both systems (maximum elevations from the mean square plane are 0.005 and 0.003 Å in **2** and **3**, respectively), the CH_3 groups being also coplanar with the rings [average $C(CH_3)$ deviations from the C_6 planes are 0.04 Å in both species]. H atoms could be directly located from the Fourier maps for both species (with some difficulty in **2**; see Experimental Section), and the CH_3 groups orientation is shown in Figures 1 and 2. While C–C(Me) bond distances are strictly equivalent in both ligands [mean 1.51 (1) and 1.504 (3) Å in **2** and **3**, respectively], the C_6 rings show major differences. It is remarkable that, in spite of the idealized *mm* symmetry, the $(1,2,4,5\text{-}C_6H_2Me_4)$ ligand shows clear "long–short" C–C bond length alternation within the ring [1.419 (3), 1.400 (3) Å]. The difference in bond length is strictly comparable to that found in both $(C_6H_6)M(CO)_3$ (0.017 Å for M = Cr at 78 K; 0.020 Å for M = Mo at 120 K)[12,13] and only slightly smaller than in $(C_6Me_6)Mo(CO)_3$ (0.036 Å).[10] The "short" C–C bonds are "trans" to the CO groups. Unfortunately, the poorer quality of the data of **2** prevents direct comparison between the two arenes. In **2**, C–C distances range from 1.38 (1) to 1.41 (1) Å and do not follow a regular pattern.

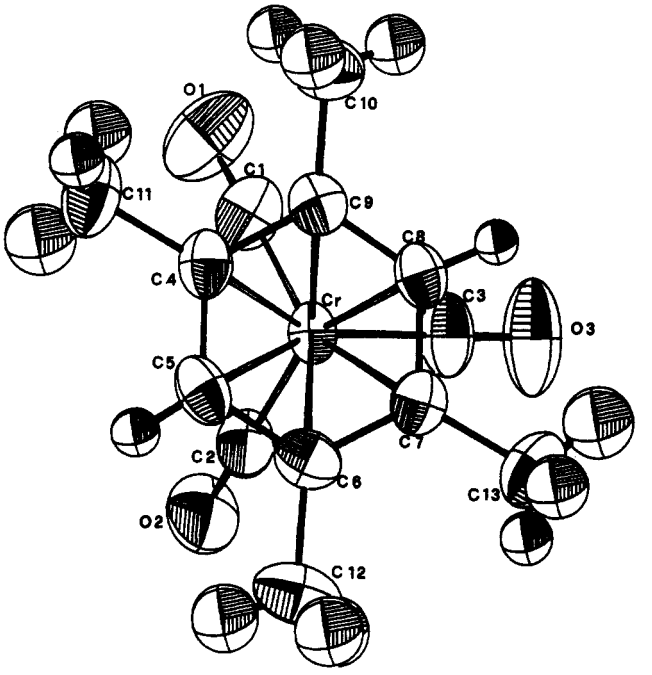

Figure 2. ORTEP projection of $(1,2,4,5\text{-}C_6H_2Me_4)Cr(CO)_3$ (**3**) showing 50% thermal ellipsoids.

Cr–C(ring) distances average 2.22 (1) and 2.220 (2) Å in **2** and **3**, respectively, and are comparable with the values found in $(C_6H_6)Cr(CO)_3$ [2.221 (8) Å at room temperature; 2.229 (2) Å at 78 K],[12] $(C_6H_5Me)Cr(CO)_3$ [2.213 (5) Å],[6a] $(C_6Me_6)Cr(CO)_3$ [2.233 (10) Å],[7] and $(C_6Et_6)Cr(CO)_3$ [2.235 (3) Å].[9] In both species the Cr atom lies almost exactly over the C_6 ring centers [Cr–C(ring) ranges 2.21 (1)–2.24 (1) and 2.203 (2)–2.232 (2) Å in **2** and **3**, respectively].

Cr–C(CO) and C–O distances average 1.82 (1), 1.15 (1) Å and 1.835 (2), 1.154 (2) Å in **2** and **3**, respectively, falling within the range of values observed in the aforementioned species. The C_6 ring plane and the plane defined by the C(CO) atoms form angles of 0.9 and 1.5° in **2** and **3**, respectively. These values are comparably smaller than that in $(C_6H_6)Cr(CO)_3$ (3.4°). However, the arene bending is an intermolecular effect, as it has been shown to increase on decreasing the temperature [4.3° in $(C_6H_6)Cr(CO)_3$ at 78 K; 4.49 and 4.96° in $(C_6H_6)Mo(CO)_3$ at room temperature and 120 K].[12,13]

Proton Relaxation Studies and Potential Energy Barrier Calculations. Figure 3a reports the log T_1 profile of **1** versus $10^3/T$ (K) as measured at 60 MHz by the inversion–recovery technique. In many features, this profile strongly resembles the one previously reported for $(C_6H_6)Cr(CO)_3$,[3i] which showed a T_1 minimum at

(7) Bailey, M. F.; Dahl, L. F. *Inorg. Chem.* **1965**, *4*, 1298.
(8) Muetterties, E. L.; Bleeke, J. R.; Wucherer, E. J.; Albright, T. A. *Chem. Rev.* **1982**, *82*, 499.
(9) Iverson, D. J.; Hunter, G.; Blount, J. F.; Damewood, J. R.; Mislow, K. *J. Am. Chem. Soc.* **1981**, *103*, 6073.
(10) Koshland, D. E.; Meyers, S. E.; Chesik, J. P. *Acta Crystallogr., Sect. B* **1977**, *33*, 2013.
(11) (a) Albright, T. A.; Hoffmann, P.; Hoffmann, R. *J. Am. Chem. Soc.* **1977**, *99*, 7546. (b) Kok, R. A.; Hall, M. B. *J. Am. Chem. Soc.* **1985**, *107*, 2599.
(12) (a) Rees, B.; Coppens, P. *Acta Crystallogr., Sect. B*, **1973**, *B29*, 2516. (b) Wang, Y.; Angermund, K.; Goddard, R.; Kruger, C. *J. Am. Chem. Soc.* **1987**, *109*, 587.
(13) Braga, D.; Grepioni, F.; Bürgi, H.-B. Manuscript in preparation.

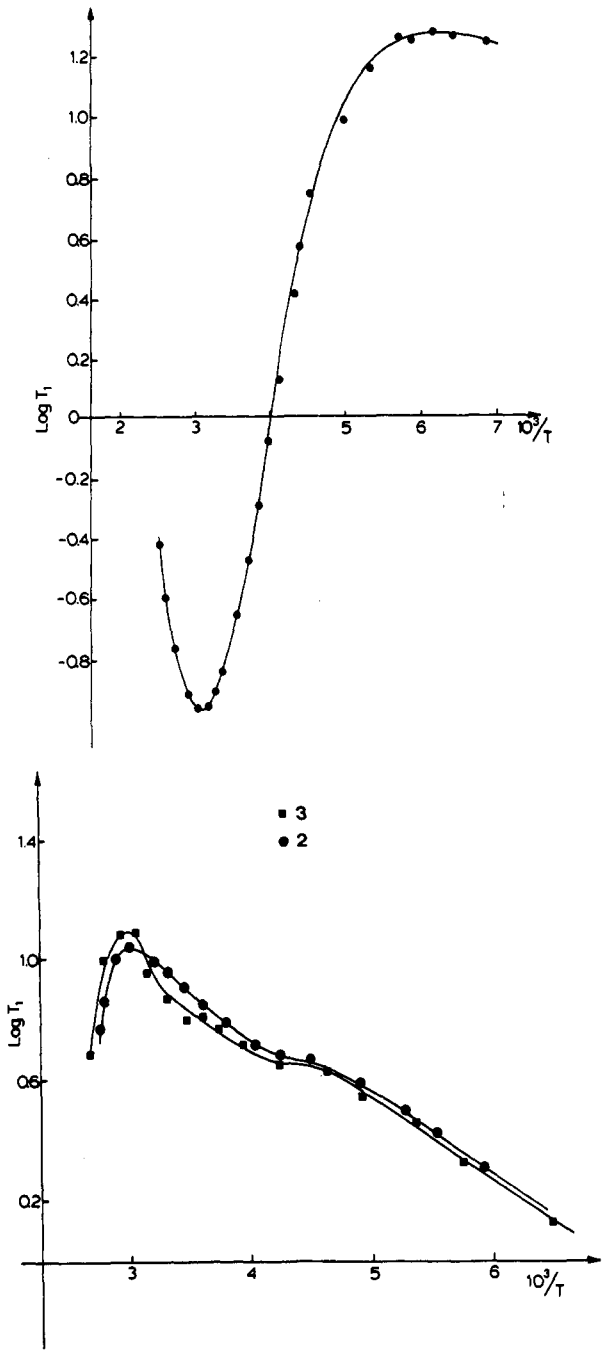

Figure 3. Plots of log T_1 versus $10^3/T$ for **1** (a, top) and for **2** and **3** (b, bottom).

182 K at the same observation frequency. It is then likely that the dynamic process that causes the T_1 minimum for **1** (at 322 K) is the rotation of the π-bonded arene fragment around its coordination axis, analogous to that observed in $(C_6H_6)Cr(CO)_3$. The activation energy associated with this process [25.9 kJ/mol, as obtained from the slope of the curve of log T_1 versus $10^3/T$ from 278 to 217 K)] is slightly larger than the corresponding value (17.6 kJ/mol) found for the rotation of the benzene ring in $(C_6H_6)Cr(CO)_3$.[3i]

From PE barrier calculations[4d] (Figure 4a), we found that the C_6Me_6 fragment appears to be able to rotate freely in the lattice at room temperature. The ΔE_{max} value of 14.2 kJ/mol is very similar to the value previously reported for the corresponding benzene derivative (18.4 kJ/mol).[4b] The $(CO)_3$ reorientation, on the contrary, encounters a very large PE barrier that does not allow jumping motion (Figure 4b). However, the bottom of the PE well is rather flat, suggesting that the $(CO)_3$ group can undergo extensive swinging motion at room temperature. Similar behavior

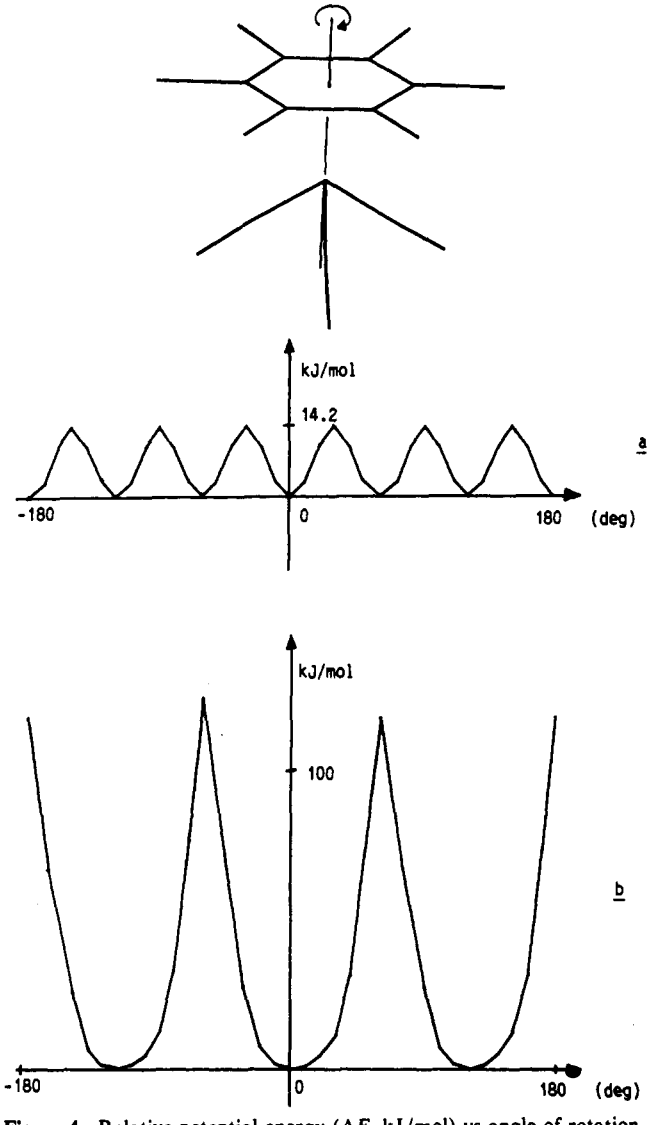

Figure 4. Relative potential energy (ΔE, kJ/mol) vs angle of rotation (deg) for reorientation of the arene ligand (a) and of the tricarbonyl group (b) in $(C_6Me_6)Cr(CO)_3$.

has been previously observed for the species $(C_6H_5Me)M(CO)_3$ (M = Cr, Mo).[4b,6b]

Although our probe does not allow us to reach temperatures below 148 K, the T_1 profile of **1** from 183 to 396 K clearly indicates that a second minimum of T_1 might be present at lower temperature. The dynamic process responsible for the reduction of T_1 in the low-temperature range is the rotation of the methyl group, which is expected to have an activation energy between 2 and 6 kJ/mol.

Let us now consider the proton log T_1 behavior versus $10^3/T$ (K) of **2** and **3** (Figure 3b). As for **1**, the spin–lattice relaxation appears to be governed by a single exponential over the entire temperature range. Although no T_1 minimum was detected in these log T_1 profiles, on the assumption that a single correlation time τ_c is dominating the modulation of the dipolar interaction in the various temperature regimes, T_1 may be interpreted by the Kubo–Tomita equation,[14] and since $\tau_c = \tau_0 \exp(E_a/RT)$, log T_1 vs $10^3/T$ (K) gives E_a/R as the slope. At low temperatures (from 210 to 150 K), the proton relaxation rates of **2** and **3** are determined by dynamic processes, whose activation energies are 5.90 and 5.23 kJ/mol, respectively. These processes may be easily assigned to the rotation of the methyl groups. The measured E_a's are in the range of values currently found for methyl group rotation in the solid state in a variety of systems.[15] We were unable on

(14) Kubo, R.; Tomita, K. *J. Phys. Soc. Jpn.* **1954**, *9*, 888.

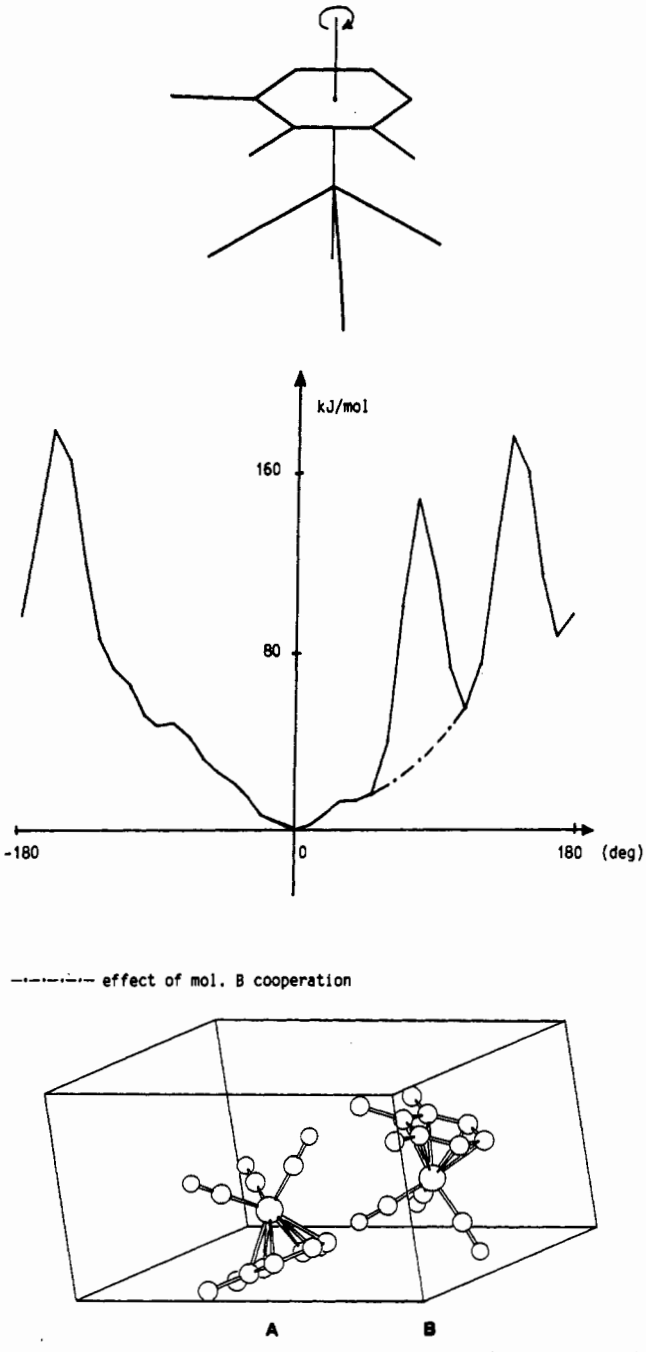

Figure 5. (a) Top: Relative potential energy (ΔE, kJ/mol) vs angle of rotation (deg) for reorientation of the arene ligand in (1,2,3-$C_6H_3Me_3$)$Cr(CO)_3$. The dotted line represents the effect of "cooperation" by the $(CO)_3$ group of molecule B. (b) Bottom: The packing relationship between molecules A and B in (1,2,3-$C_6H_3Me_3$)-$Cr(CO)_3$.

our spectrometer to get the T_1 minimum for this process (where $\tau_c\omega_0 \approx 0.62$). However, it is possible to estimate the temperature (T_{min}) at which it would be expected to occur from the simple empirical relation between E_a values and T_{min}, $E_a/RT_{min} = 10 \pm 1$, which has been recently shown to hold very well for thermally activated rotation of methyl groups. The values of T_{min} obtained in this way for **2** and **3** are 71 ± 7 and 63 ± 6 K, respectively.[29]

Above 330 K, both **2** and **3** show a drastic reduction of the observed T_1. Although only a few T_1 data may be collected before melting occurs, the drastic shortening of T_1 clearly indicates that a new dynamic process is occurring in this temperature range. The similarity of the observed behavior of T_1 for **2** and **3** with that observed for arene rotation in **1** suggests that, at these temperatures, a free rotation of the π-bonded arene groups may also occur. A further piece of information comes from PE barrier calculations, which clearly indicate that at room temperature the reorientation of the arene fragments in **2** and **3** involves very large energy barriers and is not a realistic process (see Figures 5 and 6). Reorientation of the tricarbonyl groups in both **2** and **3** is also forbidden ($\Delta E > 120$ kJ/mol).

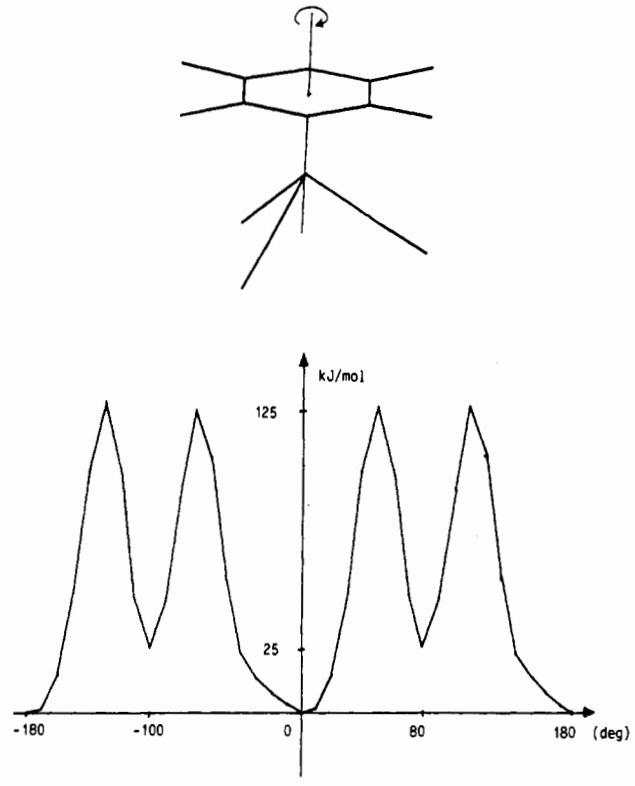

Figure 6. Relative potential energy (ΔE, kJ/mol) vs angle of rotation (deg) for reorientation of the arene ligand in (1,2,4,5-$C_6H_2Me_4$)$Cr(CO)_3$.

In order to gain insight into the effect of a temperature increase on the crystals of **2** and **3**, the behavior of the diffraction pattern as a function of the temperature was checked (see Experimental Section). Interestingly, the diffraction patterns for both **2** and **3** do not change on increasing the temperature up to ca. 333 K. Above 333 K, the crystal lattice suddenly collapses, though no melting is observed. We take this as an evidence that the crystal undergoes an order/disorder phase transition with loss of long-range order. This process is not reversible: when the temperature is decreased back to 298 K, diffraction peaks are still measurable, but neither the starting unit cells nor new ones corresponding to different ordered phases, can be obtained.

Support for the hypothesis that a phase transition occurs above 333 K was obtained by recording the DSC traces, which show for both **2** and **3** (but not for **1**) an endothermic (not reversible) peak at 338 K.

These findings suggest that, at room temperature, the complete rotation of the arene groups in **2** and **3** is forbidden in the crystal packing, while it may be achieved at higher temperature through a transition to a new phase. In these conditions the observed decrease of T_1 may be accounted in terms of a rapid (on the NMR time scale) reorientation of the arene fragments or of the entire molecules. Similar behavior has been observed in the case of substituted ferrocenyl derivatives.[16] Interestingly, **2** and **3** are in accord with the criterion forwarded by Postel and Reiss to forecast the existence of a "plastic phase",[17] falling within the condition for which $d/D > 0.81$, d being the minimum distance between molecular centers and D being the maximum diameter of the molecule ($d/D = 0.93$ and 0.91 for **2** and **3**, respectively).

(15) Eguchi, T.; Chilara, H. *J. Magn. Res.* **1988**, *76*, 143.

(16) Sato, K.; Katada, M.; Sano, H.; Konno, M. *Bull. Chem. Soc. Jpn.* **1984**, *57*, 2361.

(17) Postel, M.; Riess, J. R. *J. Phys. Chem.* **1977**, *81*, 2634.

Table II. Crystal Data and Details of Measurements for $(1,2,3\text{-}C_6H_3Me_3)Cr(CO)_3$ (**2**) and $(1,2,4,5\text{-}C_6H_2Me_4)Cr(CO)_3$ (**3**)

	2	**3**
formula	$C_{12}H_{12}CrO_3$	$C_{13}H_{14}CrO_3$
M_r	256.2	270.2
space group	$P2_1/n$ (No. 14)	$P2_1/n$ (No. 14)
T, K	298	298
a, Å	7.289 (4)	8.985 (1)
b, Å	13.114 (4)	12.527 (2)
c, Å	12.526 (3)	9.011 (1)
β, deg	97.64 (4)	118.22 (9)
V, Å^3	1186.7	1275.7
Z	4	4
$F(000)$	528	560
D_{calcd}, g cm^{-3}	1.43	1.41
λ(Mo Kα), Å	0.71069	0.71069
μ(Mo Kα), cm^{-1}	8.90	8.26
R; R_w;[a] S	0.071; 0.069; 0.68	0.032; 0.037; 1.35
k; g[a]	1.0; 0.0136	1.0; 0.0012

[a] $R_w = \sum[(F_o - F_c)w^{1/2}]/\sum F_o w^{1/2})$, where $w = k/[\sigma(F) + |g|F^2]$.

In the intermediate temperature range (from 220 to 330 K; see Figure 3) both **2** and **3** show a nonlinear behavior of $1/T_1$, which cannot be explained on the basis of the occurrence of the two dynamic processes discussed above. An additional motion could be present that, however, is unable to create a new minimum for T_1. For an appreciation of this phenomenon, it may be useful to consider again the potential energy profiles reported in Figures 5 and 6.

The PE profile for **2** (Figure 5a) is characterized by a large and rather flat bottom surrounded by steeply rising potential walls. The PE well is not symmetric with respect to the origin; on the right-hand side (+90° clockwise rotation of the arene), a "local" maximum is seen, while ΔE decreases to ca. 50 kJ/mol if the fragment is rotated further (+110°). We were able to discover that only one of the neighboring molecules (molecule B in Figure 5b) is responsible for the presence of the maximum at +90°, while the boundary PE barriers are determined by several molecules of the first neighbor shell. It is actually possible to "flatten down" the intermediate barrier by allowing a small torsional displacement of ca. ±10° of the $(CO)_3$ group belonging to molecule B, while the arene fragment is reorienting (see broken line in Figure 5b). This "cooperative" motion of the $(CO)_3$ group further enlarges the PE well, accommodating the arene fragment, which becomes able to undergo large amplitude torsional motion about its coordination axis at room temperature. The PE profile for **3** shows equivalent minima at 0 and ±180° in accord with the symmetry of the fragment. "Local" minima (ca. 25 kJ/mol) are seen after rotations of −100 and +80°, though separated by high PE barriers (see Figure 6). The effect of a cooperative motion is, however, more difficult to forecast.

In conclusion, we suggest that these large amplitude motions of the arene fragments in both **2** and **3** are responsible for the additional modulation on the dipolar field associated with the rotation of the methyl groups, which, in turn, leads to an improvement in the intermediate temperature range of the proton relaxation efficiency.

Experimental Section

Synthesis of 1–3. Compounds **1–3** were prepared according to published methods[18-20] and their purity was checked by IR spectroscopy (KBr pellets). The complete elimination of the solvent employed in the crystallization was obtained by sublimation and checked by observing the ^{1}H NMR spectra of a concentrated solution of aliquots of the sublimated sample, with $CDCl_3$ as solvent.

X-ray Structure Determination of 2 and 3. Crystal data and details of measurements for both **2** and **3** are summarized in Table II. Diffraction intensities were collected at room temperature on an Enraf-Nonius CAD-4 diffractometer equipped with Mo Kα radiation and reduced to F_o values; no decay correction was necessary. The structures were solved by direct methods, which afforded the position of the Cr atoms; all remaining atoms were located by subsequent difference Fourier syntheses. In **3**, all H atoms were also directly located. Their positions were refined by imposing equivalence of the two C(sp^2)–H distances and the C(sp^3)–H distances. H atom location was more difficult in **2**. Only the H(ring) and some of the H(Me) atoms could be found even by using a low-θ data set. The known positions were then used to put the remaining H atoms in calculated ones (H–C–H = 109.5°). Once a complete geometry was obtained, these groups were refined as rigid bodies. The structural model refinement was made by least-squares calculations, the minimized function being $\sum w(F_o - KF_c)^2$. The weighting scheme employed was $w = K/[\sigma^2(F) + |g|F^2]$, where both K and g were refined. For all calculations, the SHELX[21] package of crystallographic programs was used with the analytical scattering factors, corrected for the real and imaginary parts of anomalous dispersion, taken from ref 22. All atoms were allowed to vibrate anisotropically, except the H atoms, which were treated isotropically in **3**. Two isotropic U values were otherwise refined

Table III. Fractional Atomic Coordinates for **2**

atom	x	y	z
Cr	0.83474 (10)	0.19190 (6)	0.23469 (7)
C(1)	0.7381 (8)	0.1080 (5)	0.1270 (5)
O(1)	0.6809 (8)	0.0522 (5)	0.0600 (5)
C(2)	0.7255 (7)	0.1117 (4)	0.3261 (5)
O(2)	0.6540 (7)	0.0595 (4)	0.3826 (4)
C(3)	0.6243 (9)	0.2695 (5)	0.2138 (7)
O(3)	0.4924 (9)	0.3176 (5)	0.1966 (8)
C(4)	1.0483 (9)	0.2498 (7)	0.3633 (7)
C(5)	0.9983 (11)	0.3274 (5)	0.2909 (9)
C(6)	1.0102 (9)	0.3133 (5)	0.1803 (8)
C(7)	1.0721 (8)	0.2205 (5)	0.1449 (6)
C(8)	1.1236 (6)	0.1424 (4)	0.2189 (5)
C(9)	1.1100 (7)	0.1565 (5)	0.3288 (5)
C(10)	1.0851 (14)	0.2072 (9)	0.0262 (7)
C(11)	1.1987 (10)	0.0424 (6)	0.1826 (7)
C(12)	1.1652 (10)	0.0759 (7)	0.4112 (6)

Table IV. Fractional Atomic Coordinates for **3**

atom	x	y	z
Cr	0.18370 (3)	0.08824 (2)	0.79572 (2)
C(1)	0.1142 (2)	0.1285 (2)	0.9306 (2)
O(1)	0.0650 (2)	0.1545 (2)	1.0134 (1)
C(2)	0.3668 (2)	0.1671 (1)	0.8294 (2)
O(2)	0.4826 (2)	0.2176 (1)	0.8504 (2)
C(3)	0.3033 (3)	−0.0117 (1)	0.8744 (2)
O(3)	0.3769 (3)	−0.0756 (1)	0.9210 (2)
C(4)	−0.0482 (2)	0.1512 (1)	0.6964 (1)
C(5)	0.0867 (2)	0.1725 (1)	0.6384 (2)
C(6)	0.1931 (2)	0.0989 (1)	0.6053 (2)
C(7)	0.1638 (2)	0.0013 (1)	0.6317 (1)
C(8)	0.0264 (2)	−0.0197 (1)	0.6901 (1)
C(9)	−0.0801 (2)	0.0522 (1)	0.7226 (1)
C(10)	−0.2260 (3)	0.0243 (2)	0.7817 (2)
C(11)	−0.1576 (3)	0.2324 (2)	0.7266 (2)
C(12)	0.3326 (3)	0.1278 (2)	0.5397 (2)
C(13)	0.2704 (3)	−0.0812 (2)	0.5998 (2)
H(1)	0.108 (2)	0.233 (1)	0.615 (1)
H(2)	0.026 (2)	−0.084 (1)	0.718 (1)
H(3)	−0.312 (2)	0.027 (2)	0.717 (1)
H(4)	−0.231 (2)	0.065 (1)	0.848 (1)
H(5)	−0.193 (2)	−0.030 (1)	0.834 (2)
H(6)	−0.081 (2)	0.284 (1)	0.753 (2)
H(7)	−0.263 (2)	0.232 (1)	0.677 (1)
H(8)	−0.170 (2)	0.223 (2)	0.809 (1)
H(9)	0.364 (2)	0.192 (1)	0.555 (2)
H(10)	0.325 (2)	0.102 (2)	0.463 (1)
H(11)	0.438 (2)	0.109 (2)	0.577 (2)
H(12)	0.263 (2)	−0.139 (1)	0.648 (2)
H(13)	0.230 (2)	−0.104 (1)	0.524 (1)
H(14)	0.387 (2)	−0.061 (1)	0.612 (2)

(18) Fisher, E. O.; Öfele, K.; Essler, H.; Frölich, W.; Mortensen, P.; Semmlinger, W. *Chem. Ber.* **1958**, *91*, 2763.
(19) Price, J. T.; Sorensen, T. S. *Can. J. Chem.* **1968**, *46*, 515.
(20) Razuaev, G. A.; Kutzenetsov, V. A.; Egorochkin, A. N.; Klimov, A. A.; Artenov, A. N.; Sirotkin, N. I. *J. Organomet. Chem.* **1977**, *128*, 213.
(21) Sheldrick, G. M. SHELX76. Program for Crystal Structure Determination. University of Cambridge, Cambridge, England, 1976.
(22) *International Tables for X-ray Crystallography*; Kynoch Press: Birmingham, England, 1975; Vol. IV, pp 99–149.

Table V. Parameters for the Atom–Atom Potential Energy Calculations (kcal/mol)[a]

	A	*B*	*C*
H···H	4900	4.29	29.0
C···C	71600	3.68	421.0
O···O	77700	4.18	259.4
CH_3···CH_3[b]	4580	2.26	2980.0
Cr···Cr	270600	3.28	3628.0

[a] For crossed interactions: $A = (A_xA_y)^{1/2}$, $B = (B_x + B_y)/2$, and $C = (C_xC_y)^{1/2}$. [b] CH_3···CH_3 and Cr···Cr interactions were treated as Cl···Cl and Kr···Kr interactions, respectively (see text).

for the H(ring) and H(Me) of **2** [0.10 (1) and 0.16 (1) Å^2, respectively].

Fractional atomic coordinates for **2** and **3** are reported in Tables III and IV, respectively.

The behavior with the temperature of the crystals of **2** and **3** was checked by heating the crystals with a stream of warm N_2 from an Enraf-Nonius cryostat. The temperature was increased in 5 K steps; at each temperature value the intensities of 25 well-centered reflections were measured, and their angular settings were used for unit cell refinement. In both cases, the unit volumes showed a steady increase with temperature up to 333 K. Crystal lattice collapse was observed to occur for both crystals between 333 and 338 K. The experiment was repeated on fresh crystals in order to check its reproducibility.

Potential Energy Barrier Calculations. The calculations of the potential energy barriers associated with the arene and tricarbonyl groups reorientations in the solid state are based on a Buckingham potential of the type

$$PE = \sum_i \sum_j (Ae^{-Br_{ij}} - Cr_{ij}^{-6})$$

where index i runs over all atoms of the reference molecule and index j over the atoms of the surrounding molecules distributed according to crystallographic symmetry. The quantity r_{ij} represents the atom–atom intermolecular distance.[23] The values of the coefficients A, B, and C used in this work are listed in Table V.[24] For Cr and Mo, such coefficients are not available; values for the corresponding noble gases (Kr and Xe) were used. In all calculations a 10-Å cutoff distance was used; extension of the summation beyond this limit did not change the results appreciably. Ionic contributions were not considered.

All calculations were performed by using a slightly modified version of the computer program OPEC.[25] Methyl groups in all species were treated as Cl atoms (see Table V) centered on the C(Me) positions. This was made necessary to take into account the almost free rotational motion of the CH_3 groups in the solid and is justified by the similarity of the bulk of the CH_3 and Cl groups.[26]

In all cases, arene and/or tricarbonyl reorientations were performed around the coordination axes (those passing through the middle of the C_6 rings and the metal atom or through the mass center of the $(CO)_3$ group and the metal atom). The potential energy was calculated at 10° rotational steps for complete rotations of the fragments between ±180°.

Relative potential energy profiles (ΔE) were calculated as ΔE = PE-PE(min), where PE(min) is the value corresponding to the observed structure (0° rotation). The intermolecular [ΔE(inter)] and intramolecular [ΔE(intra)] contributions were calculated separately. ΔE(tot) was obtained as ΔE(inter) + ΔE(intra). In all cases, ΔE(intra) was found to be very small (<4 kJ/mol) indicating that intramolecular nonbonding interactions play a limited role in the control of the reorientational processes. As a consequence, ΔE(tot) is almost completely determined by the intermolecular interactions. No cooperation or relaxation of the molecules surrounding the reorienting fragment was allowed ("static environment" approximation).[27]

T_1 Measurements. Spin–lattice relaxation times were measured on a Stelar Spin Master spectrometer operating at 60 MHz, by using the inversion–recovery pulse sequence (d–180°–t–90°), where d is the delay time ($d > 5T_1$) and t is a variable time. The 90° pulse width was 11 μs. T_1 was calculated by means of a two-parameter nonlinear least-squares program by using at least 10 different t values.[28]

The temperature was maintained within ±2 K by a nitrogen gas flow (low temperatures) or air (high temperatures). The experimental temperature was checked by a thermocouple set in the sample tube just over the sample (≈80 mg) under examination.

DSC Measurements. Differential scanning calorimetry (DSC) was carried on with a Du Pont DSC cell driven by a thermal analyzer unit at a heating rate of 10 K min^{-1} in a flowing atmosphere of N_2.

Acknowledgment. Financial support by the Ministero della Pubblica Istruzione is acknowledged.

Supplementary Material Available: Tables of anisotropic thermal parameters, fractional atomic coordinates and thermal parameters, fractional atomic coordinates for the hydrogen atoms, and complete bond distances and angles for **2** and **3**, respectively (23 pages); F_o/F_c tables for **2** and **3**, respectively (27 pages). Ordering information is given on any current masthead page.

(23) (a) Pertsin, A. J.; Kitaigorodski, A. I. *The atom-atom potential method*; Springer-Verlag: Berlin 1987. (b) Gavezzotti, A.; Simonetta, M. *Organic Solid State Chemistry*; Desiraju, G. R., Ed.; Elsevier: Amsterdam, 1987.

(24) (a) Mirsky, K. *Computing in Crystallography, Proceedings of the International Summer School on Crystallographic Computing* Delft University Press: Twente, The Netherlands, 1978; p 169. (b) Gavezzotti, A.; Simonetta, M. *Chem. Rev.* **1981**, *82*, 1.

(25) Gavezzotti, A. OPEC. Organic Packing Potential Energy Calculations. University of Milano, Milan, Italy. See also: Gavezzotti, A. *J. Am. Chem. Soc.* **1983**, *195*, 5220.

(26) Gavezzotti, A. *Nouv. J. Chim.* **1982**, *6*, 443.

(27) Gavezzotti, A.; Simonetta, M. *Acta Crystallogr., Sect. A* **1976**, *32*, 997.

(28) Doddrell, D. M.; Bendall, M. R.; O'Connor, A. J.; Pegg, D. T. *Aust. J. Chem.* **1977**, *30*, 943.

(29) Very similar values were obtained for T_{min} by evaluating the magnitude of the magnetic interaction C responsible for the relaxation process:

$$C = (9\gamma^4\hbar^2)/20r^6 \quad (1)$$

Taking an interprotonic r distance equal to 1.755 Å, C becomes 8.77×10^9 rad s^{-2}. By linear regression of the function of log T_1 vs $10^3/T$ (K) we get $C\tau_0$ and E_a. The T_1 minimum then occurs according to eqs 2 and 3. T_{min}'s become equal to 65.5 and 58.9 K for **2** and **3**, respectively.

$$\omega\tau_c = \omega\tau_0 \exp(E_a/RT_{min}) = 0.62 \quad (2)$$

$$1/T_{min} = (R/E_a) \ln (0.62\omega\tau_0) \quad (3)$$